Impacts of Minimum Technical Requirements and IBR Control Strategies on Power System Performance: A WECC 240-bus Case Study

Xue Lyu[1], Andy Hoke[2], Di Wu[1], Ross Guttromson[3], Brett A Ross[1], Shuan Dong[2]
[1]Pacific Northwest National Laboratory, Richland, USA
[2]National Laboratory of the Rockies, Golden, USA
[3]Sandia National Laboratories, Albuquerque, USA

***Abstract*—The growing penetration of inverter-based resources (IBRs) introduces challenges for power system stability and protection because IBR behavior is highly dependent on control design. Grid codes such as IEEE 2800-2022 specify minimum performance requirements for IBRs, including frequency ride-through (FRT) and voltage ride-through (VRT). This paper uses time-domain simulations on the WECC 240-bus system to quantify how (i) FRT/VRT relay settings, (ii) active-power headroom, and (iii) reactive current injection affect post-fault voltage/frequency recovery and generation tripping. Results show that headroom and enhanced reactive injection improve damping and reduce trips, with the largest benefits for grid-following (GFL) IBRs. Grid-forming (GFM) controls provide stronger voltage support and more robust fault recovery, with increasing advantages at higher IBR penetration. These findings inform ongoing revisions of ride-through and control requirements.**

***Index Terms*—Grid codes, IBRs, voltage ride-through, frequency ride-through, grid-following control, grid-forming control.**

I. Introduction

The increasing penetration of inverter-based resources (IBRs) in modern power systems is changing the dynamic performance of the power grid, which was previously designed and operated based on the physical characteristics of synchronous machines. According to their control philosophy, IBRs can be categorized into two types: grid-following (GFL) and grid-forming (GFM). GFL IBRs operate as controlled current sources that follow the grid voltage and frequency. In contrast, GFM IBRs act as controlled voltage sources that establish grid voltage and frequency, exhibiting voltage controlled dynamics similar to synchronous machines.

Accurate inverter models are essential for analyzing their impact on power system stability and performance. However, acquiring complete visibility into inverter models and control algorithms is challenging, as vendors are understandably reluctant to disclose intellectual property-protected technology [1]. Therefore, generic models that are vendor-independent are essential for use as standardized templates in comprehensive system studies, enabling consistent analysis across different inverter technologies and manufacturers. The Western Electricity Coordinating Council (WECC) Modeling and Validation Subcommittee (MVS) has developed generic IBR models for both GFL and GFM controls that can be used to assess the impact of IBRs on grid stability and overall system performance.

To facilitate the seamless integration of IBRs, consensus based performance requirements are needed. Standards such as IEEE 2800-2022 establish minimum technical requirements (MTR) for interconnection and interoperability of IBRs connecting to transmission and sub-transmission systems [2]. The IEEE 1547 series of standards establishes requirements for interconnection and interoperability of distributed energy resources [3], [4]. However, the system level impacts of these requirements often lack rigorous technical justification. For example, relaxing frequency ride-through (FRT) and voltage ride-through (VRT) requirements may reduce implementation burden, whereas strengthening them could enhance bulk power system reliability in high IBR scenarios. As the working groups continue to refine IEEE 1547 and IEEE 2800, targeted dynamic simulations of the future bulk power system's response to reliability events are needed to inform the appropriate stringency of these requirements. Moreover, IEEE 2800-2022 primarily reflects grid-following IBRs implementations; explicit, standardized performance requirements for grid-forming IBRs have not yet been established.

To address these gaps and inform future standards development, we develop an automated framework that configures, parameterizes, and evaluates IBR control settings in the modified WECC 240-bus model via positive-sequence simulations in PSS/E. To evaluate the impact of ride-through requirements, we implement FRT and VRT relay logic at IBR connection buses, parameterized per IEEE 2800-2022 and IEEE 1547-2003. The key contributions of this work are: (1) an automated PSS/E-based simulation framework for evaluating IBR integration impacts in large-scale systems; (2) a systematic assessment of how IEEE 1547-2003 vs. IEEE 2800-

This material is based upon work supported by the U.S. Department of Energy, Office of Critical Minerals and Energy Innovation (CMEI). Pacific Northwest National Laboratory is operated for the DOE by Battelle Memorial Institute under Contract DE-AC05-76RL01830. National Laboratory of the Rockies is operated for the DOE under Contract DE-AC36-08GO28308. The views expressed in the article do not necessarily represent the views of the DOE or the U.S. Government. The U.S. Government retains and the publisher, by accepting the article for publication, acknowledges that the U.S. Government retains a nonexclusive, paid-up, irrevocable, worldwide license to publish or reproduce the published form of this work, or allow others to do so, for U.S. Government purposes.

979-8-3315-8138-1

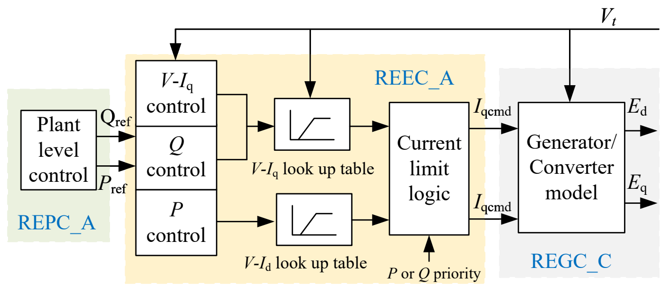

Fig. 1. Modeling GFL IBRs in PSSE/E.

2022 FRT/VRT settings and active power headroom influence post-fault voltage/frequency recovery and generator tripping in the WECC 240-bus system; and (3) a comparative analysis of GFL versus GFM controls, including the effects of enhanced reactive current injection, on system-level post-fault response and stability margins.

II. Generic IBRs models

A. GFL Model

The WECC Renewable Energy Modeling Task Force (REMTF) developed second generation generic models for renewable energy systems (RES)—including wind and PV—across the major commercial software platforms used for North American power system studies [5], [6]. In this work, we represent GFL RES using the standard combination of REPC_A, REEC_A, and REGC_C: REPC_A provides plant level control and generates active/reactive power references; REEC_A translates these references into active and reactive current commands; and REGC_C implements the voltage source converter interface with inner current control loops and a phase-locked loop (PLL) to inject the commanded currents into the grid. The control structure is shown in Fig. 1.

REPC_A, REEC_A, and REGC_C offer multiple configurable control flags, including voltage control, Q control, power factor control, $P - f$ droop control, Q–V droop, active/reactive power priority modes, and PLL enable/disable options. Parameter settings of each model can follow the guidance provided in [7].

B. GFM Model

In this work, we use the WECC Modeling and Validation Subcommittee–approved REGFM_A1 model [8] to represent GFM RES. The inverter phase angle is set by a $P - f$ droop controller. To provide active power support while respecting limits, a PI based limiter constrains P within $P_{\max}, P_{\min}$. The inverter terminal voltage magnitude is regulated using a $Q-V$ droop characteristic with reactive-power limits. An optional VFlag enables a PI controller to directly regulate the point-of-connection voltage. In this paper, VFlag is enabled; therefore, the IBRs operate in PCC voltage-regulation mode.

During normal operation, the droop controller regulates the inverter phase angle and voltage magnitude. During faults, the current limiting is activated and the current magnitude is capped at $I_{\max}$ and the current angle is remain unchanged, and then inverter terminal voltage is formed by,

$$E\angle\delta = V_t\angle\delta_t + I_{\max}\angle\varphi(R + jX), \tag{1}$$

where E is the formed voltage magnitude, δ is the formed inverter phase angle, V_t and δ_t are the inverter terminal voltage and angle, ϕ is the inverter current angle, and R, X are the inverter coupling resistance and reactance. φ can be expressed as,

$$I_{\max}\angle\varphi = \frac{E_{\text{droop}}\angle\delta_{\text{droop}} - V_t\angle\delta_t}{R + jX}. \tag{2}$$

III. IBR Minimum Technical Requirements Implementation

IBRs are required to provide essential grid services to maintain power system stability and reliability. MTRs are specified in IEEE standards to ensure IBRs can deliver these services effectively. For example, IEEE 2800-2022 specifies comprehensive requirements including reactive power capability, voltage and reactive power control modes, primary frequency response, and response to abnormal operating conditions. To fulfill the requirements specified in IEEE 2800-2022, IBR control parameters are configured as follows: (i) primary frequency control is activated with a 5% P–f droop characteristic for both GFL and GFM inverters, (ii) the reactive power-voltage droop coefficient is set to 0.3 p.u. in the REPC_A and REGFM_A1 models, and (iii) the reactive power capability, $Q_{\max} = 0.33$ p.u., $Q_{\min} = -0.33$ p.u. for both GFL and GFM IBRs.

To assess the impact of differing FRT/VRT requirements, we model ride-through protections using the built-in PSS/E generator trip relay models VTGTPAT (under/over-voltage) and FRQTPAT (under/over-frequency). These relay models are added to the system .dyr file at the corresponding generator connection buses. The relay settings are parameterized according to IEEE 2800-2022 and IEEE 1547-2003. Overall, IEEE 2800-2022 specifies more stringent ride-through requirements. Note that IEEE 2800-2022 does not mandate high-voltage ride-through above 1.2 p.u.; to enable direct comparison with IEEE 1547-2003, we cap exposure above 1.2 p.u. at 0.16 s. A similar modification is applied for frequencies below 57 Hz. IEEE 1547-2003 allows adjustable FRT times ranging from 0.16 s to 300 s for frequencies between 57 Hz and 59.8 Hz; in this study, we set the FRT time within this band according to Western Interconnection generator settings specified in NERC PRC-024 [9]. The implemented IBR FRT/VRT relay settings, shown in Fig. 2, enforce compliance with the respective ride-through requirements and enable evaluation of their system-level impacts on stability and post-fault recovery.

FRT/VRT relays are also applied to conventional generators in the WECC 240-bus system, with settings based on frequency and voltage ride-through boundaries for the Western Interconnection as specified in NERC PRC-024 [9].

A Python script has been developed to modify PSS/E dynamics (.dyr) files, adjust IBR parameters, and add FRT/VRT

979-8-3315-8138-1

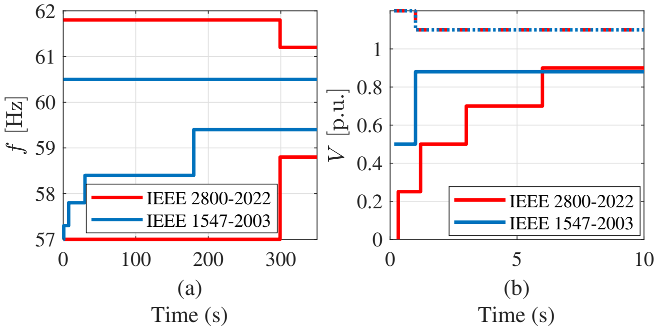

Fig. 2. Ride-through relay model settings for IBRs: (a) FRT relay settings, (b) VRT relay settings.

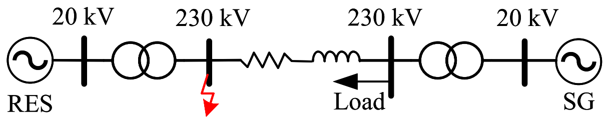

Fig. 3. Configuration of the single-IBR single-SG test system.

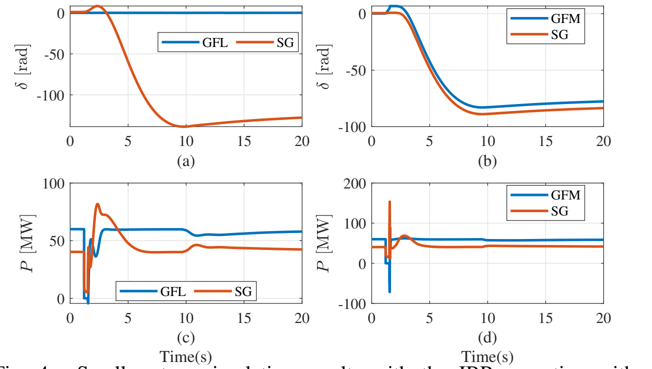

Fig. 4. Small-system simulation results with the IBR operating without reserve (MPPT).

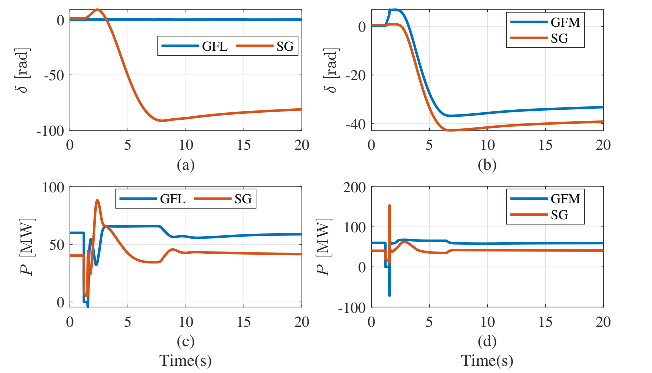

Fig. 5. Small-system simulation results with the IBR providing 10% active-power reserve.

relay models for both IBRs and SGs, facilitating MTR implementation.

IV. Case Studies

A. Study in a small system

We first test a three-phase bolted short circuit in a single-IBR single-SG system, shown in Fig.3. The IBR is modeled either as a GFL controller using REPC_A–REEC_A–REGC_C, or as a GFM controller using REGFM_A1. A three phase bolted fault is applied at the high voltage bus and cleared after 320 ms. Transmission faults typically clear within 100 ms; this scenario represents delayed clearing, as might occur with a failed circuit breaker or a communication link failure. Two scenarios are considered: (i) the IBR has no active power reserve (operates at maximum power point tracking, MPPT), and (ii) the IBR has a 10% active power reserve. The reserve is implemented by adjust $P_{\max}$ in the plant/electrical models (REPC_A/REEC_A for GFL and REGFM_A1 for GFM). For the no reserve case, the phase angle and active power of the IBR and SG are shown in Fig. 4. In the GFL+SG case, the post fault phase angle mismatch between the IBR and SG is large, leading to a significant variation in SG active power: it rises, then drops, and finally returns to its pre-fault value. In contrast, in the GFM+SG case the IBR and SG phase angles track closely and the post-fault active power recovery is faster. Results for the 10% reserve case are shown in Fig. 5. Compared with the no reserve case, both GFL and GFM configurations demonstrate exhibit smaller post fault angle excursions and slightly faster active power recovery both the IBR and the SG.

B. Study in the WECC 240-bus system

A modified WECC 240-bus system developed by NREL is used as the test bed. The California area has high renewable penetration. In the base power flow case, 183 generators are in service with a total output of about 150 GW; of these, 104 are IBR units producing approximately 47.7 GW, corresponding to a renewable penetration of about 31.8%.

The control settings for GFL and GFM IBRs follow the configurations described in Section III. The maximum current limit $I_{\max}$ is set to 1.1 p.u. for all IBRs. For GFM IBRs, the VFlag is enabled. For GFL IBRs, we first enable voltage control in the REPC_A and REEC_A models with Q priority control activated. Post-fault performance is evaluated by (i) identifying tripped generation using a post-processing script that flags units whose active power is nonzero prior to the disturbance and drops to zero by the end of the simulation, (ii) calculating the average damping ratio of post fault voltage oscillations in the 0.1–3 Hz frequency range using the Hilbert transform method, and (iii) checking whether system frequency remains below 59.3, 59.2, 59.0, 58.8, or 58.6 Hz for more than 10 s, which would trigger underfrequency load shedding (UFLS). For (ii), for each bus we form the post-fault voltage deviation $x_i(t) = V_i(t) - V_{i,0}$, where $V_{i,0}$ is the pre-fault average voltage. The deviation is band-pass filtered to 0.1–3 Hz, and the oscillation envelope is obtained from the analytical signal magnitude $A_i(t) = |x_i(t) + j\mathcal{H}\{x_i(t)\}|$. An exponential fit $A_i(t) \approx A_0 e^{-\sigma t}$ yields the decay rate σ; the dominant frequency f_d is estimated from the filtered signal ($\omega_d = 2\pi f_d$). The damping ratio is computated as $\zeta_i = \frac{\sigma}{\sqrt{\sigma^2+\omega_d^2}}$. The reported average damping ratio is the mean of ζ_i across buses with valid oscillatory responses.

1) Comparison of IBR control modes and reserve levels under IEEE 1547-2003 FRT/VRT requirements: A three phase bolted fault (320 ms) is applied at bus 2404 to evaluate four scenarios: GFL and GFM controls without/with 10% active power reserve under IEEE 1547-2003 FRT/VRT requirements.

979-8-3315-8138-1

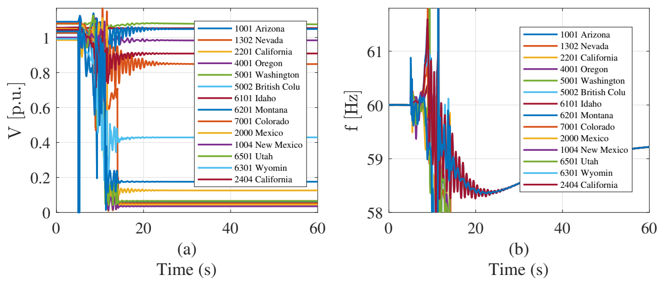

Fig. 6. Response under IEEE 1547-2003 FRT/VRT settings with IBRs operating without reserve (GFL: REPC_A–REEC_A–REGC_C). (a) voltage magnitude at selected buses (14 representative area buses plus the faulted bus), (b) frequency at the same buses.

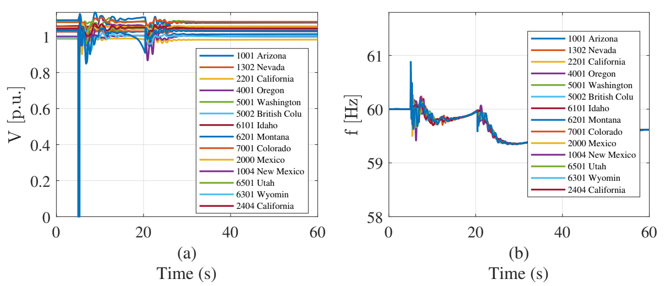

Fig. 7. Response under IEEE 1547-2003 FRT/VRT settings with 10% IBR reserve (GFL: REPC_A–REEC_A–REGC_C). (a) voltage magnitude at selected buses (14 representative area buses plus the faulted bus), (b) frequency at the same buses.

The voltage and frequency responses at representative buses across different areas of the WECC 240-bus system (14 area buses plus the faulted bus) are shown in Figs. 6-9, with post-fault evaluations summarized in TableI. It can be found that GFL without reserve exhibits the worst performance with 93.23 GW generation tripped (>50% of total) and over half the buses failing voltage recovery, indicating system instability. This outcome is driven by poor post-fault voltage recovery and limited active-power support (no headroom), which together trigger widespread VRT relay operations and subsequent IBR/SG tripping, resulting in a cascading loss of support. With 10% reserve, the GFL case improves substantially but still trips 8.9 GW of generation and exhibits low average voltage damping ratios. Several IBRs/SGs trip during the recovery period (approximately 5–13 s), and a delayed trip of the IBR at Bus 3932 (around 20.4 s) causes a secondary frequency dip before the system settles to a new steady state. In contrast, both GFM scenarios reach a stable post-fault steady state. The reserve case further reduces generation tripping and achieves noticeably higher voltage damping ratios than the GFL cases. However, all four scenarios fail to meet IEEE 2800-2022 requirements for damping ratio ≥ 0.3, highlighting the challenges of achieving adequate damping under severe transmission-level faults.

2) Comparison of IBR Control Modes and Reserve Levels under IEEE 2800-2022 FRT/VRT Requirements: To evaluate the impact of IBR control strategies and active power reserves, the same three-phase bolted fault was applied at bus 2404 under IEEE 2800-2022 FRT/VRT settings. Table III presents the system performance for different combinations of IBR

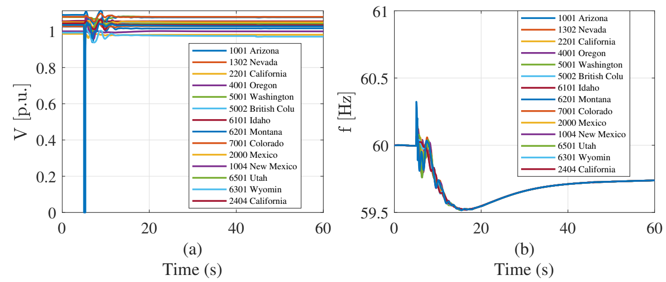

Fig. 8. Response under IEEE 1547-2003 FRT/VRT settings with IBRs operating without reserve (GFM: REGFM_A1). (a) voltage magnitude at selected buses (14 representative area buses plus the faulted bus), (b) frequency at the same buses.

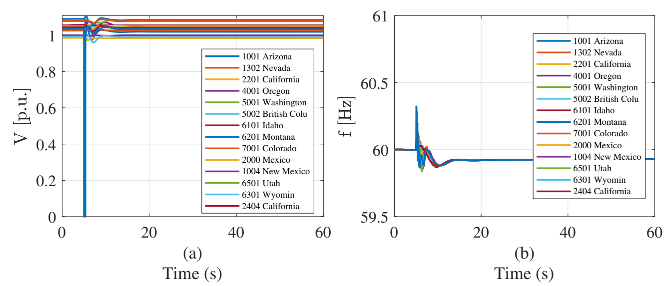

Fig. 9. Response under IEEE 1547-2003 FRT/VRT settings with 10% IBR reserve (GFM: REGFM_A1). (a) voltage magnitude at selected buses (14 representative area buses plus the faulted bus), (b) frequency at the same buses.

control modes and reserve levels. Key findings include: (i) Active power reserve significantly improves GFL performance, transforming the system from post fault instability to stable operation with only 4.83 GW of generation tripped; (ii) GFM controls exhibit superior and consistent performance (0.543 GW tripped) with minimal sensitivity to reserve availability; and (iii) GFM configurations achieve faster system recovery and significantly higher damping ratios compared to GFL, demonstrating enhanced grid stability under severe fault conditions. Notably, in the GFL no-reserve case, tripped generation is higher than in the corresponding IEEE 1547-2003 case because post-fault voltages recover slowly and remain in the moderate-undervoltage region. While IEEE 2800-2022 allows longer ride-through at very low voltage, it includes additional recovery-region limits (e.g., $V < 0.9$ p.u. for 6 s) that are exceeded in this scenario, leading to more IBR trips and a larger cascading loss of support.

3) Effect of Reactive Current Injection Characteristics of GFL IBRs on System Performance: In the GFL model, enabling the V–I_q function in REEC_A increases the com-

TABLE I
SYSTEM PERFORMANCE WITH IBR FRT/VRT SETTINGS PER IEEE 1547-2003.

Case Description	Tripped Generation (GW)	Average Voltage Damping Ratio	UFLS Triggered
GFL, no reserve	93.23	N/A	Yes
GFL, 10% headroom	8.96	0.0651	No
GFM, no reserve	4.40	0.126	No
GFM, 10% headroom	3.03	0.218	No

979-8-3315-8138-1

TABLE II
SYSTEM PERFORMANCE WITH IBR FRT/VRT SETTINGS PER IEEE 2800-2022.

Case Description	Tripped Generation (GW)	Average Voltage Damping Ratio	UFLS Triggered
GFL, no reserve	146.18	N/A	Yes
GFL, 10% headroom	4.83	0.110	No
GFM, no reserve	0.543	0.203	No
GFM, 10% headroom	0.543	0.244	No

manded reactive current during low-voltage conditions. In this study, $V{-}I_q$ control is enabled with proportional gain $K_{qv} = 2$ and PI freezing at voltage extremes (<0.5 or >1.1 p.u.); thus, when the terminal voltage drops below 0.5 p.u., the controller rapidly drives reactive current injection toward its limit, accelerating voltage restoration after fault clearing. Table III shows that aggressive reactive injection improves performance in three scenarios: system stability is achieved under IEEE 2800-2022 without reserve, and generation tripping is reduced with 10% reserve under IEEE 1547-2003 relay settings. The damping ratios in these three cases are improved. However, the IEEE 1547-2003 no-reserve case remains unstable, indicating that enhanced reactive support alone cannot overcome the limitations of legacy FRT/VRT requirements when no active power reserve is available.

TABLE III
SYSTEM PERFORMANCE WITH GFL IBRS ENABLING $V - I_q$ CONTROL.

Case Description	Tripped Generation (GW)	Average Voltage Damping Ratio	UFLS Triggered
GFL, no reserve, 1547-2003	99.0	N/A	Yes
GFL, 10% headroom, 1547-2003	7.83	0.130	No
GFL, no reserve, 2800-2022	11.19	0.116	Yes
GFL, 10% headroom, 2800-2022	4.83	0.125	No

4) Higher IBR Penetration Scenario: A higher-IBR-penetration scenario was created by replacing selected coal-fired synchronous generators with IBRs (by updating the .sav and .dyr files), increasing the total IBR penetration to approximately 47.4%. Because the coal units' synchronous-machine models are removed, this scenario has lower inertia than the base case. With all IBRs configured with 10% active power reserve, the system's dynamic performance under high penetration is evaluated using the same 320 ms bolted fault at bus 2404. Table IV summarizes the performance metrics for different IBR control modes and protection standards. The results reveal significant differences in scalability between control modes: (i) GFL performance degradation: The system loses stability under both IEEE 2800-2022 and IEEE 1547-2003 settings due to excessive generation tripping following the fault, indicating that GFL controls do not scale effectively with higher IBR penetration levels. (ii) GFM robustness: In contrast, GFM-controlled IBRs maintain the same level of generation tripping as observed in the baseline 31.8% penetration case, demonstrating superior scalability and system support capability at higher penetration levels. Note that these results are based on positive-sequence RMS simulation; EMT studies would be useful to assess sub-cycle converter phenomena that may influence the immediate post-fault behavior in weak-grid, high-IBR conditions.

TABLE IV
SYSTEM PERFORMANCE WITH HIGH IBR PENETRATION (47.4%).

Case Description	Tripped Generation (GW)	Average Voltage Damping Ratio	UFLS Triggered
GFL, 1547-2003	100.1	N/A	Yes
GFL, 2800-2022	140.9	N/A	Yes
GFM, 1547-2003	3.07	0.231	No
GFM, 2800-2022	0.543	0.246	No

V. CONCLUSION

This work develops an automated simulation framework for integrating IBRs into large scale power grids and uses it to assess how minimum technical requirements in IEEE 2800-2022, particularly FRT/VRT, affect system performance following short circuit faults in the WECC 240-bus system. Simulations show that relaxing FRT/VRT settings increases the risk of generator tripping. Provisioning active power headroom materially improves post-fault recovery, with the greatest benefits for GFL IBRs. For GFL controls, voltage control design is important: faster, higher magnitude reactive current injection during faults accelerates voltage restoration. GFM IBRs provide stronger voltage support and damping than GFL controls, yielding more robust fault recovery and reduced sensitivity to ride-through parameter variations; these advantages grow with IBR penetration. These results highlight the need to coordinate ride-through protection, IBR headroom policies, reactive current response, and control strategy selection, and can inform future standards development.

REFERENCES

[1] B. B. Johnson, T. Roberts, O. Ajala, A. D. Domínguez-García, S. V. Dhople, D. Ramasubramanian, A. Tuohy, D. Divan, and B. Kroposki, "A generic primary-control model for grid-forming inverters: Towards interoperable operation & control." in *HICSS*, 2022, pp. 1–10.

[2] "IEEE standard for interconnection and interoperability of inverter-based resources (IBRs) interconnecting with associated transmission electric power systems," *IEEE Std 2800-2022*, pp. 1–180, 2022.

[3] "IEEE standard for interconnecting distributed resources with electric power systems," *IEEE Std 1547-2003*, pp. 1–28, 2003.

[4] "IEEE standard for interconnection and interoperability of distributed energy resources with associated electric power systems interfaces," *IEEE Std 1547-2018 (Revision of IEEE Std 1547-2003)*, pp. 1–138, 2018.

[5] P. Pourbeik, "Model user guide for generic renewable energy system models," *Electric Power Research Institute*, 2015.

[6] Electric Power Research Institute, "Model user guide for generic renewable energy system models," Electric Power Research Institute, Palo Alto, CA, Tech. Rep. 3002027129, 2023. [Online]. Available: https://www.epri.com/research/products/000000003002027129

[7] PJM, "PJM dynamic model development guidelines for interconnection analysis," https://www.pjm.com/-/media/dotcom/planning/services-requests/pjm-dynamic-model-development-guidelines.ashx, 2024.

[8] W. Du, "Model specification of droop-controlled, grid-forming inverters (REGFM_A1)," Pacific Northwest National Laboratory (PNNL), Richland, WA (United States), Tech. Rep., 2023.

[9] NREC, "PRC-024-4: Transmission-connected resources — frequency and voltage protective relay settings," https://www.nerc.com/pa/Stand/202002_Transmissionconnected_Resources_DL/2020-02_PRC-024-4_Clean_03272024.pdf, 2024.

979-8-3315-8138-1